Stereospecificity of Substrate Usage by Glyoxalase 1: Nuclear Magnetic Resonance Studies of Kinetics and Hemithioacetal Substrate Conformation

ARTICLE *in* BIOCHEMISTRY · APRIL 1994

Impact Factor: 3.02 · DOI: 10.1021/bi00178a011 · Source: PubMed

4 AUTHORS, INCLUDING:

Caroline Rae
University of New South Wales
118 PUBLICATIONS **2,720** CITATIONS
SEE PROFILE

Philip W Kuchel
University of Sydney
308 PUBLICATIONS **5,153** CITATIONS
SEE PROFILE

Biochemistry 1994, *33*, 3548–3559

Stereospecificity of Substrate Usage by Glyoxalase 1: Nuclear Magnetic Resonance Studies of Kinetics and Hemithioacetal Substrate Conformation†

Caroline Rae,‡ Séan I. O'Donoghue,§ William A. Bubb, and Philip W. Kuchel*

Department of Biochemistry, The University of Sydney, Sydney 2006, Australia

Received November 16, 1993®

ABSTRACT: The specificity of glyoxalase 1 for the diastereomers of its hemithioacetal substrate [which forms spontaneously between an α-keto aldehyde and reduced glutathione (GSH)] was investigated by exploiting the differences between their ^{1}H NMR spectra at pH* 4.4. The ^{1}H NMR spectra of the hemithioacetals of glutathione with phenylglyoxal or methylglyoxal were assigned with the aid of conventional decoupling and two-dimensional NMR spectroscopic techniques. The rate of interconversion of the diastereomers was determined at 30 °C from the results of an inversion-transfer technique and found to be 0.30 ± 0.04 s^{-1} (± sd) in the case of phenylglyoxal and 0.15 ± 0.02 s^{-1} in the case of methylglyoxal. Stereopreference of the enzyme was tested by the addition of large amounts of yeast glyoxalase 1 to a reaction mixture; glyoxalase 1 preferentially operated on one diastereomer of the phenylglyoxal hemithioacetal but the diastereomers of methylglyoxal appeared to be operated upon indiscriminately. From computer models of the kinetics of possible reaction schemes, a mechanism involving glyoxalase 1 catalysis of both diastereomers of the hemithioacetals was shown to be the most consistent with the experimental data. Estimates of internuclear distances in the diastereomers, obtained from 2D NMR spectra were used in "dynamical simulated annealing" calculations to generate likely structures of the substrates. Relative ring-current shifts obtained from 1D NMR spectra were used, together with a ring–current shift algorithm, to select structures with compatible conformations. We conclude that the rate of conversion of substrate by the enzyme is dependent upon the *overall* conformation of the substrate molecule, rather than merely its stereochemical configuration (*R* or *S*).

Glyoxalase 1 (*S*-D-lactoylglutathione methylglyoxal-lyase (isomerizing); EC 4.4.1.5) is an exceptional enzyme in that it produces a stereochemically unambiguous product, *S*-D-acylglutathione (Ekwall & Mannervik, 1973; Patterson *et al.*, 1981), from a diastereomeric mixture of rapidly interconverting hemithioacetals (Figure 1) which are formed spontaneously by reaction between an α-keto aldehyde, such as methyl- or phenylglyoxal, and reduced glutathione (GSH;[1] Racker, 1951). The question whether glyoxalase 1 converts one of these stereoisomers preferentially has been the subject of several investigations (*e.g.*, Brown *et al.*, 1981; Griffis *et al.*, 1983; Landro *et al.*, 1992), as this is related to the mechanism of this anticancer target enzyme (Vince & Wadd, 1969). However, experimentally, it is a difficult problem to address, due to the rapid spontaneous interconversion of the diastereomers.

At pH* (unadjusted meter reading) 4.4 the diastereomers of the hemithioacetal (HTA) of phenylglyoxal and GSH are in sufficiently slow exchange on the NMR time scale for some resonances arising from each to be distinguished by ^{1}H NMR at 100 MHz (Brown *et al.*, 1981). The latter authors noted differential disappearance of the methine proton resonances of the phenylglyoxal-HTA after addition of glyoxalase 1, and concluded that the enzyme was using one of the diastereomers preferentially, perhaps even exclusively, although the data did not allow resolution of this question. This idea was challenged by Griffis *et al.* (1983) who, using isotope-labeling techniques, concluded that glyoxalase 1 from yeast and porcine erythrocytes used both diastereomers of phenylglyoxal hemithioacetal, although they were not able to determine, to their satisfaction, whether or not the diastereomers were converted with equal rates.

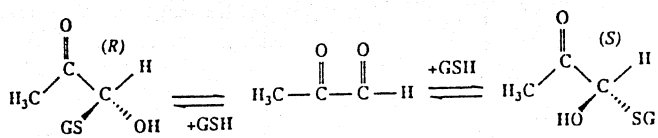

FIGURE 1: Interconversion of methylglyoxal/GSH hemithioacetal diastereomers. GSH is L-γ-glutamyl-L-cysteinyl glycine.

The initial mechanism proposed for the reaction involved a hydride shift (Frazen 1956; Rose, 1957) but more recent work supports the existence of a *cis*-enediol intermediate, with the reaction proceeding via a general base-catalyzed, fast "shielded proton" transfer (Hall *et al.*, 1976, 1978; Shinkai *et al.*, 1981; Chari & Kozarich, 1982; Kozarich *et al.*, 1981; Chari & Kozarich, 1983; Douglas *et al.*, 1985). The existence of a *cis*-enediol intermediate (Chari & Kozarich, 1983) seemed to support the idea of stereoselective conversion of the substrate; the *cis*-enediol being derived from the *S*-configuration of the HTA (Brown *et al.*, 1981). Griffis *et al.* (1983), upon observing lack of stereopreference by glyoxalase 1, proposed

† This work was supported by a grant from the Australian National Health and Medical Research Council to P.W.K. C.R. was supported by an NH & MRC Postgraduate Research Scholarship. The simulation control program was developed by Duke University, Durham, NC, with support from NIH Grant RR01693.

‡ Present address: Department of Biochemistry, The University of Oxford, South Parks Rd., Oxford, OX1 3QU UK.

§ Present address: EMBL, Meyerhofstr. 1, D-6900, Heidelberg, Germany.

* Author to whom correspondence should be directed.

® Abstract published in *Advance ACS Abstracts*, February 1, 1994.

[1] The abbreviations used are as follows: GSH, reduced glutathione; pH*, unadjusted pH meter reading; HTA, hemithioacetal; NMR, nuclear magnetic resonance; DQFCOSY, double-quantum filtered correlation spectroscopy; NOESY, nuclear Overhauser enhancement spectroscopy; NOE, nuclear Overhauser effect; DSA, dynamical simulated annealing; SCoP, simulation control program.

0006-2960/94/0433-3548$04.50/0

a mechanism involving enzyme-catalyzed interconversion of the bound diastereomeric hemithioacetals (*R* to *S*) before the product was formed by isomerization.

However, recent work by Landro *et al.* (1992), using the stereochemically "locked" substrate analogues (*R*)- and (*S*)-glutathiolactaldehyde, supports a mechanism whereby both diastereomers are able to act as substrates, although not with quite the same affinity. It is hypothesized that in the reaction a proton is abstracted non-stereoselectively, followed by stereospecific reprotonation at the adjoining carbon. The authors quoted examples of two other enzymes known to act in a similar stereorandom/stereospecific manner, as well as previous work with the "inverted" substrate (glutathiomethyl)-glyoxal (Kozarich & Chari, 1982), in support of this hypothesis.

In the work presented here, the NMR spectral differences between hemithioacetal diastereomers at pH* 4.4 of both phenylglyoxal-HTA, and methylglyoxal-HTA (the "natural" substrate of glyoxalase 1) were exploited to allow a semi-quantitative kinetic analysis of the time course of the enzyme-catalyzed reaction. The rates of interconversion of the diastereomers were measured using an inversion–transfer NMR technique and the values of the rate constants incorporated into a computer model of the reaction sequence(s). This enabled us to explore whether the enzyme was employing the diastereomers preferentially, or not. Furthermore, the spectral differences observed were used, along with results of 2D NMR studies and distance–geometry calculations, to establish the configuration in aqueous solution of the diastereomeric substrates, and to rationalize the effect of this spatial configuration upon the rate of the enzyme-catalyzed reaction.

Theory. Observed stereopreferential usage of substrate by glyoxalase 1 (Brown *et al.*, 1981; Landro *et al.*, 1992) can give rise to a number of possible models for catalysis. HTA(*R*) and HTA(*S*) denote the stereoisomers of the hemithioacetal and P denotes the product, *S*-D-acylglutathione. The simplest models are as follows:

(1) The enzyme converts only one diastereomer (presumed to be the *S* form) to product, *viz.*,

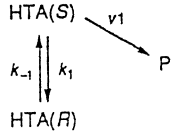

(1)

where the hemithioacetals are subject to rapid chemical interconversion with first-order rate constants k_1 and k_{-1}. Glyoxalase 1 is assumed to obey Michaelis-Menten kinetics, with the rate $v1$, depending on a V_{max} and a K_M value.

(2) Glyoxalase 1 converts both diastereomers to product and may, or may not show stereopreference. Different V_{max} and K_M values would be required for each Michaelis-Menten equation describing the reaction velocities $v1$ and $v2$

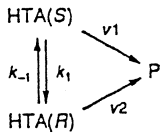

(2)

(3) Glyoxalase 1 may obey the mechanism proposed by Griffis *et al.* (1983), where the enzyme *catalyzes* interconversion of bound diastereomers before their conversion to product

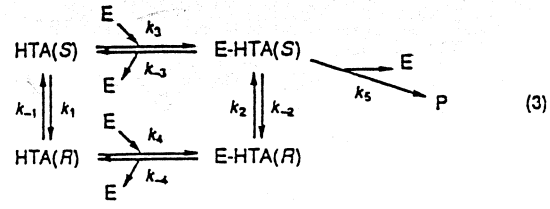

(3)

The rate constants k_2 and k_{-2} characterize the enzyme-catalyzed interconversion of the enzyme-bound hemithioacetals. The rate constants k_3, k_{-3}, k_4, and k_{-4} characterize the binding of the hemithioacetal to the enzyme, and the isomerization of substrate to product is characterized by the rate constant k_5. Note that in all cases, although the enzyme-catalyzed reaction has been shown to be reversible (Sellin & Mannervik, 1983), the reverse reaction is several orders of magnitude slower than that of the forward reaction so its rate constant was set to zero in the present work.

MATERIALS AND METHODS

Materials. Methylglyoxal was obtained as the dimethyl acetal from Aldrich Chemical Co., Milwaukee, WI, hydrolyzed by the method of Kellum *et al.* (1978), and purified by distillation under reduced pressure (Rae *et al.*, 1990). Phenylglyoxal monohydrate was also supplied by Aldrich. GSH and glyoxalase 1 (Grade X from yeast) were purchased from the Sigma Chemical Co., St. Louis, MO. Glyoxalase 1 was used without further purification. Although glyoxalase 2 is present in this powder preparation, no NMR signals attributable to the product of this enzyme were seen during the time in which the reaction was monitored (~60 s). To the best of our knowledge, the buffer salt (citrate) in this preparation is not known to affect the reaction rate of glyoxalase 1. ^2H_2O was obtained from the Australian Institute for Nuclear Science and Engineering, Lucas Heights, NSW, Australia.

Sample Preparation. All samples contained 20–200 mM GSH and 20–400 mM α-keto aldehyde and were constituted in either 90% H_2O/10% ^2H_2O (v/v) or ^2H_2O. The pH* was altered to 4.4 using NaOH or NaO^{2}H as required. Samples containing high concentrations of phenylglyoxal were routinely filtered through an Amicon 2-μm filter to remove undissolved material.

NMR Spectrometry. All ^{1}H NMR spectra were obtained at 600.14 or 400.13 MHz on Bruker AMX-600 or AMX-400 wb spectrometers, respectively, with the variable-temperature units set to 303 K. Chemical shifts are expressed relative to external sodium 3-(trimethylsilyl)-2,2,3,3-tetradeuteriopropionate in ^2H_2O but were routinely referenced to the cysteinyl α-proton (δ 4.565) of GSH, which was present in slight excess in all samples. Assignment of the spectra was aided by selective decoupling, double-quantum filtered correlation spectroscopy (DQFCOSY), and nuclear Overhauser effect spectroscopy (NOESY) experiments. Chemical shifts and coupling constants were optimized by iterative analysis using the program NUMARIT (Quirt & Martin, 1971; further modified by W. J. E. Parr and R. A. Sebastian, Dept. of Chemistry, University of Manitoba, Winnipeg, Canada) run on a Bruker X32 work station. For the determination of chemical shifts of the γ-glutamyl protons, the spectra were iterated with average values of published coupling constants for GSH as input (Podányi & Reid, 1988). Root-mean-square deviations between calculated and experimental transitions were less than 0.1 Hz except for the γ-glutamyl subspectra where the largest

error was 0.37 Hz. ^{13}C NMR spectra were obtained at 150.92 MHz and 303 K using WALTZ-16 (Shaka *et al.*, 1983) decoupling of protons, with the decoupler gated off during the acquisition of "fully coupled" spectra. 2D heteronuclear–correlation spectra (Bax *et al.*, 1983) were acquired with delays of 3.7 and 100 ms to optimize one-bond and long-range correlations, respectively.

Hemithioacetal Interconversion Rates. The rate of interconversion of hemithioacetals was measured by acquiring inversion–transfer spectra (Robinson *et al.*, 1985) of each hemithioacetal methine proton resonance, from a solution containing ~20 mM of the diastereomers in ^2H_2O. A range of mixing times from 0 to 1.5 s was used. The data were analyzed according to the method of Perrin and Engler (1990).

Time Course of Glyoxalase I Reaction. Initial ^1H NMR spectra were obtained from samples containing ~200 mM GSH and 200 mM methylglyoxal, or ~200 mM phenylglyoxal, in ^2H_2O. Varying amounts of yeast glyoxalase 1 (500 units dissolved in 0.4 mL of ^2H_2O) were added to the sample (sufficient to give a rate of product formation greater than the rate of chemical interconversion of the stereoisomers) and a series of spectra of one or two transients each, was acquired with 16K data points. The time between adding the glyoxalase 1 and acquiring the first spectrum was minimised by modification of the sample eject assembly on the NMR magnet to permit more rapid lowering of the sample. The pulse program was compiled while the field-frequency lock was established and the magnetic field homogeneity improved. With these adaptations, the first spectrum was routinely acquired 30–40 s after addition of the enzyme. Loss of enzyme activity, due to the low pH*, has been reported to be negligible over the time period of the experiment [~2 min (Brown *et al.*, 1981)]. This experiment was repeated with increased enzyme concentrations until the reaction was too fast to monitor using NMR; in other words, until the extent of the reaction exceeded ~20% in 40 s.

Two-Dimensional Spectra. Solutions of 200 mM GSH, mixed with 300 mM phenylglyoxal or 400 mM methylglyoxal, were constituted in reverse-osmosis water (10% ^2H_2O v/v). A DQFCOSY spectrum (Piantini *et al.*, 1982), derived from 2K data points × 512 spectra of 64 transients each, was transformed with weighting by a shifted sine bell ($\theta = \pi/2$) in both F_1 and F_2 dimensions. NOESY spectra (Kumar *et al.*, 1980) were derived from 2K data points × 400 spectra of 64 transients each in the case of phenylglyoxal, and 4K data points × 512 spectra of 64 transients each in the case of methylglyoxal. The mixing times were 0.95 and 0.9 s, respectively. The spectra were transformed with one degree of zero filling using a shifted sine bell ($\theta = \pi/2$) in both the F_1 and F_2 dimensions and the peaks were integrated using the standard Bruker software (UXNMR).

Structure Determination. Peak integrals, obtained from NOESY spectra, were converted into approximate upper limits of distances by setting the integral of the cys $\beta\beta'$ cross peak to 1.8 Å (Braun *et al.*, 1981). In the case of the phenylglyoxal-HTA, where some resonances of each diastereomer were sufficiently well resolved for "chemical exchange cross peaks" to be distinct from the NOE cross peaks, the integral of the exchange peak was added to that of the corresponding NOE cross peak. Three upper distance categories were used in the structure calculations: 2.8, 3.3, and 4.5 Å. Non-NOE constraints (>4.5 Å) were used for proton pairs which lacked cross peaks in the NOESY spectrum.

Three-dimensional structures were generated from the distance constraints using the *ab initio* dynamical simulated annealing (DSA) protocol of Nilges *et al.* (1988). Since this protocol is described in detail in the X-PLOR 3.0 manual (Brunger, 1992), only a brief description is given here: The atoms were initially assigned random coordinates and initial energy minimization was carried out with the geometry terms assigned low weights compared with the nonbonded repulsive ("repel") term. Velocities were then assigned randomly at 1000 K and the dynamic trajectory of the system was calculated over ~5 ps while the weight of the energy terms was increased. The system was then "cooled" to 300 K in 50 K steps over 30 ps, and finally 200 cycles of "Powell" energy minimization were used. The calculations were run on a SUN SPARC station 2GX and the output structures were displayed on a Silicon Graphics IRIS 4D/20 workstation using the MidasPlus software package (Ferrin *et al.*, 1988).

The method of Johnson and Bovey (1958) was used to predict the magnitude of ring current shifts for each structure of phenylglyoxal-HTA generated by the DSA procedure. The predicted chemical shifts ($S_{p,i}$, $i = 1, ..., N$) were compared with the corresponding observed values ($S_{o,i}$) using the χ goodness of fit measure:

$$\chi = \frac{1}{N}\sum_{i=1}^{N}|(S_{p,i} - S_{o,i})/S_{o,i}| \qquad (4)$$

The chemical shifts that were used were those relative to the same protons in the methylglyoxal-HTA. Ideally, shifts would be compared with those of a cyclohexadiene/GSH hemithioacetal to allow for any inductive effects of the ring, but the degree of precision required here did not necessitate use of such a compound. Only the chemical shifts of the Hα, Hβ, and Hγ protons of the γ-glutamyl, and the Hβ protons of the substituted cysteinyl were used in the analysis, where the inductive effects contributed proportionately less to the overall chemical shift. The other cysteinyl protons had chemical shift differences too large to be explained largely by a ring-current effect; here, the inductive effects of the ring contribute a larger proportion of the chemical shift.

Computer Modeling. Simulations of chemical reactions shown in eqs 1 and 2 were performed with the simulation control program SCoP (Duke University, Durham, NC). Differential equations describing the reaction schemes were input to the program and the time course of the reaction was simulated using various values of rate constants, including those obtained experimentally. In the case of eq 3, the time course of the reaction was also simulated using a separate program that used a third-order Runge-Kutta, semi-implicit integrator (Gear, 1969) to generate a table of concentrations of each species with respect to time. The latter algorithm was used because the differential equations were very "stiff"; very small time increments were accompanied by very large changes in some concentrations, thus requiring extremely small step-sizes to be used in the numerical integration.

RESULTS

Figure 2 shows a 600.14-MHz ^1H NMR spectrum of a solution containing phenylglyoxal and GSH in ^2H_2O at pH* 4.4. The spectrum contains resonances assigned to five species present in the solution: phenylglyoxal monohydrate and bishydrate, the two diastereomers of the hemithioacetal (HTA), and a small amount of free GSH. Each diastereomer gave distinctly separate resonances from all protons which are differentiated in the spectrum as belonging to either diastereomer "A" or "B".

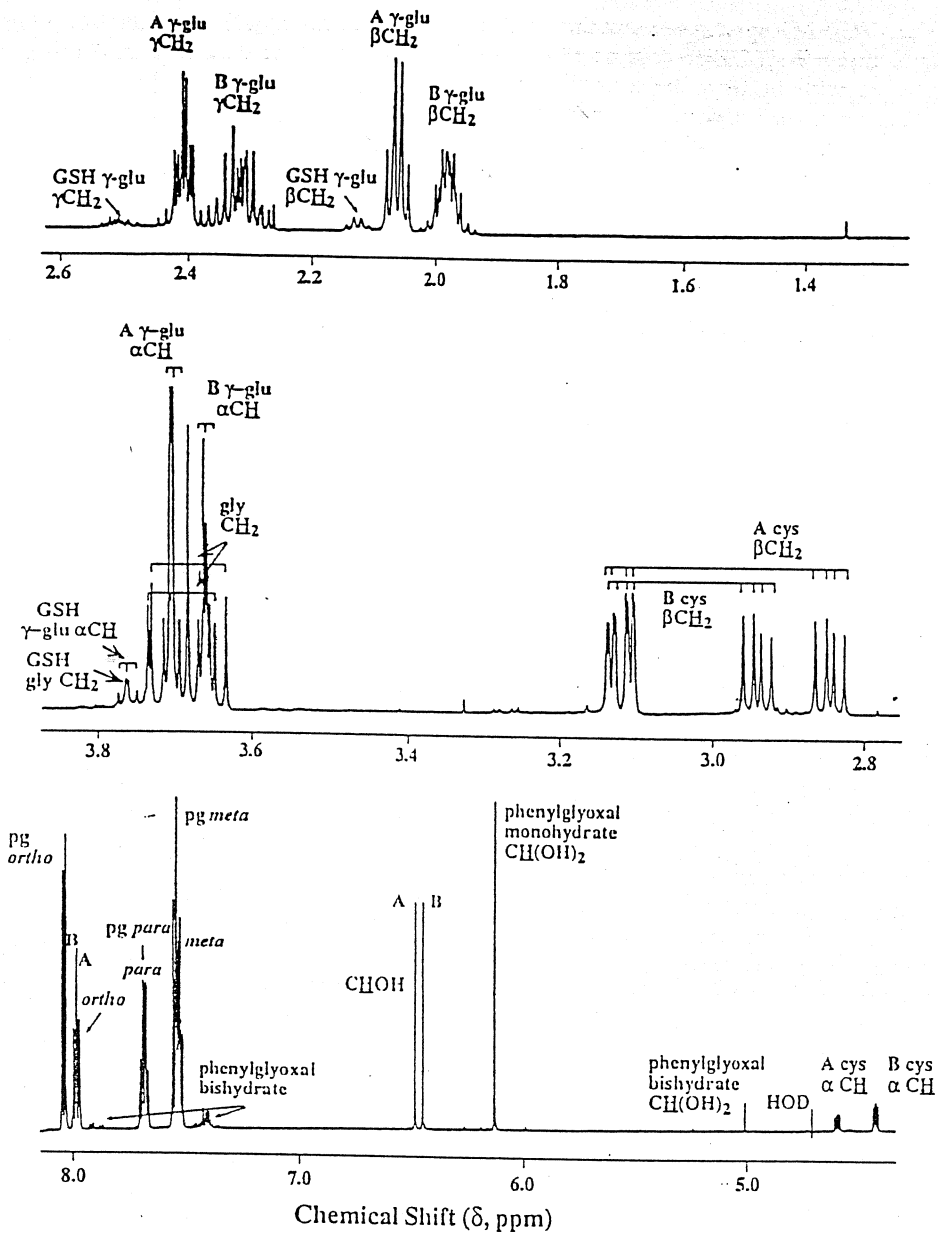

FIGURE 2: A 600.14-MHz ^{1}H NMR spectrum of phenylglyoxal and GSH at pH* 4.4. The sample contained 20 mM GSH and excess phenylglyoxal constituted in ^2H_2O; the pH* was adjusted with NaO^{2}H. The spectrum was derived from 32 transients collected over 32K data points and transformed with one degree of zero filling. Notes on assignments: The two separate hemithioacetal diastereomers were assigned as either "A" or "B". HTA A: CHOH, δ 6.507; γglu αCH, δ 3.729; γglu βCH$_2$, δ 2.094; γglu γ,γ′ CH$_2$, δ 2.428, δ 2.447; cys αCH, δ 4.617; cys β,β′ CH$_2$, δ 2.868, 3.137, $^2J_{\beta\beta'} = -14.11$ Hz, $^3J_{\alpha\beta} = 8.60$ Hz, $^3J_{\alpha\beta'} = 4.72$ Hz. HTA B: CHOH, δ 6.471; γglu αCH, δ 3.682; γglu β,β′CH$_2$, δ 1.999, 2.021; γglu γ,γ′ CH$_2$, δ 2.328, δ 2.365; cys αCH, δ 4.446; cys β,β′ CH$_2$, δ 2.962, 3.140, $^2J_{\beta\beta'} = -14.20$ Hz, $^3J_{\alpha\beta} = 8.64$ Hz, $^3J_{\alpha\beta'} = 5.20$ Hz. HTA A and B: gly CH$_2$, δ 3.675, δ 3.739, $^2J = -17.16$ Hz and δ 3.697, δ 3.742, $^2J = -17.25$ Hz (not unequivocally assignable to either species A or B). The intensity of the cys αCH protons is reduced due to presaturation of the nearby resonance, HOD. The aromatic protons of the hemithioacetal and phenylglyoxal monohydrate (pg) are labeled according to their positions in each molecule.

In the corresponding ^{13}C NMR spectrum (150.92 MHz; not shown) many of the hemithioacetal carbon atoms were also affected by the differential effect of a ring–current shift. The chemical shift assignments were as follows: HTA A; γ-glu αCH, δ 55.797, $^1J_{CH} = 142.6$ Hz; γ-glu βCH$_2$, δ 28.894, $^1J_{CH} = 132.1$ Hz; γ-glu γCH$_2$, δ 34.130, $^1J_{CH} = 129.0$ Hz; γ-glu COO$^-$, δ 176.564; γ-glu CO, δ 177.379; cys αCH, δ 56.919, $^1J_{CH} = 145.9$ Hz; cys βCH$_2$, δ 32.888, $^1J_{CH} = 143.0$ Hz; cys CO, δ 174.146; gly αCH$_2$, δ 45.878, $^1J_{CH} = 139.7$ Hz; gly COO$^-$, δ 178.406; acetal CH(OH) δ 77.391, $^1J_{CH} = 162.13$. For HTA B: γ-glu αCH, δ 55.734; γ-glu βCH$_2$, δ 28.894; γ-glu γCH$_2$, δ 34.051; γ-glu COO$^-$, δ 176.519; γ-glu CO, δ 177.227; cys αCH, δ 56.919; cys βCH$_2$, δ 32.414; cys CO, δ 174.190; gly αCH$_2$, δ 45.878; gly COO$^-$, δ 178.406; acetal CH(OH) δ 77.445; the $^1J_{CH}$ values were not significantly different from those of HTA A.

The 600.14-MHz ^{1}H NMR spectrum of a solution of methylglyoxal and GSH (Figure 3) displayed much less difference between the chemical shifts of the diastereomers; in this case the best-resolved resonances were from protons close to the chiral (*R* or *S*) carbon.

A section of the 600.14-MHz NOESY spectrum of phenylglyoxal and GSH is shown in Figure 4. Positive NOEs (negative cross peaks) were observed for 33 out of the 78 possible interactions between the 13 resolved peaks lying along the diagonal of the spectrum. The spectrum displayed NOE connections between nuclei in the same molecule, as well as cross peaks which are consistent with those arising from chemical exchange between the different isomers. For example a positive cross peak (–ve NOE) was observed between cys NH in one diastereomer and the cys NH in the other. A negative cross peak (+ve NOE) was observed between cys

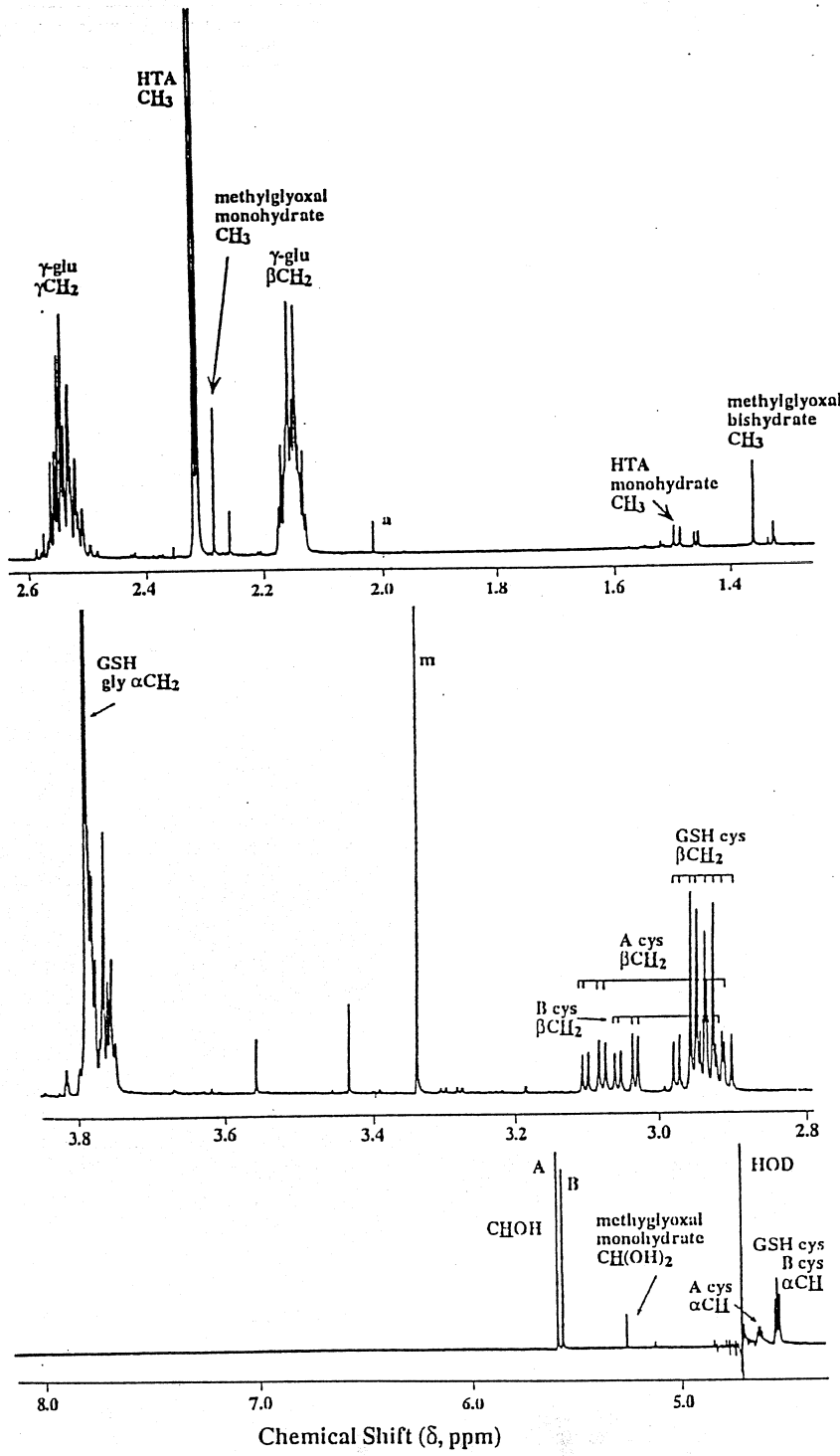

FIGURE 3: A 600.14-MHz ^1H NMR spectrum of methylglyoxal and GSH at pH* 4.4. The sample contained 20 mM GSH and excess methylglyoxal constituted in ^2H_2O; the pH* was adjusted with NaO^2H. The spectrum was derived from 32 transients collected over 32K data points and transformed with one degree of zero filling. Notes on assignments: Two separate hemithioacetal diastereomers (designated A and B) were evident from the spectra but it was not possible, on the basis of NMR spectral data alone, to assign the resonances to the specific diastereomers. The coupled cysteinyl resonances were determined by spin-decoupling experiments but the γ-glutamyl assignments could be interchanged and the relative chemical shifts are for one possible solution to the spectrum: CH_3CO, δ 2.322 and 2.316; $CH_3C(OH)_2$, δ 1.495 and 1.484; CHOH, δ 5.589 and 5.566, γglu αCH, δ 3.773; γglu βCH_2, δ 2.160; γglu γ,γ′ CH_2, δ 2.523, δ 2.551, and γglu αCH, δ 3.766; γglu βCH_2, δ 2.150; γglu γ,γ′ CH_2, δ 2.513, δ 2.533; cys αCH, δ 4.569; cys β,β′ CH_2, δ 2.940, 3.090, $^2J_{\beta,\beta'}$ = −13.98 Hz, $^3J_{\alpha\beta}$ = 8.36 Hz, $^3J_{\alpha\beta'}$ = 5.25 Hz, and cys αCH, δ 4.644; cys β,β′ CH_2, δ 2.931, 3.045, $^2J_{\beta,\beta'}$ = −14.07 Hz, $^3J_{\alpha\beta}$ = 8.43 Hz, $^3J_{\alpha\beta'}$ = 4.82 Hz; gly CH_2, δ 3.779, δ 3.802, ^2J = −17.31 Hz, and δ 3.784, δ 3.802, ^2J = −17.39 Hz. The intensity of the cys αCH protons is reduced due to presaturation of the nearby HOD resonance; a refers to the resonance from the methyl protons of acetone (δ 2.02), m to methanol (δ 3.34). The singlets at δ 3.44, 3.56, and 2.26 arise from unhydrolyzed methylglyoxal dimethyl acetal.

NH in one diastereomer and γ-glu γ CH_2 in the other diastereomer (Figure 4). Both "exchange" peaks arose from the rapid spontaneous chemical interconversion that takes place during the relatively long mixing time (0.95 s) of the NOESY experiment. The integrals of the exchange peaks were added to the integrals of the appropriate NOE peaks, thus yielding an *estimate* of the NOE that was compensated for the loss of intensity brought about by the exchange.

The chemical shifts of the A and B diastereomers of phenylglyoxal HTA were resolved, and separate NOESY

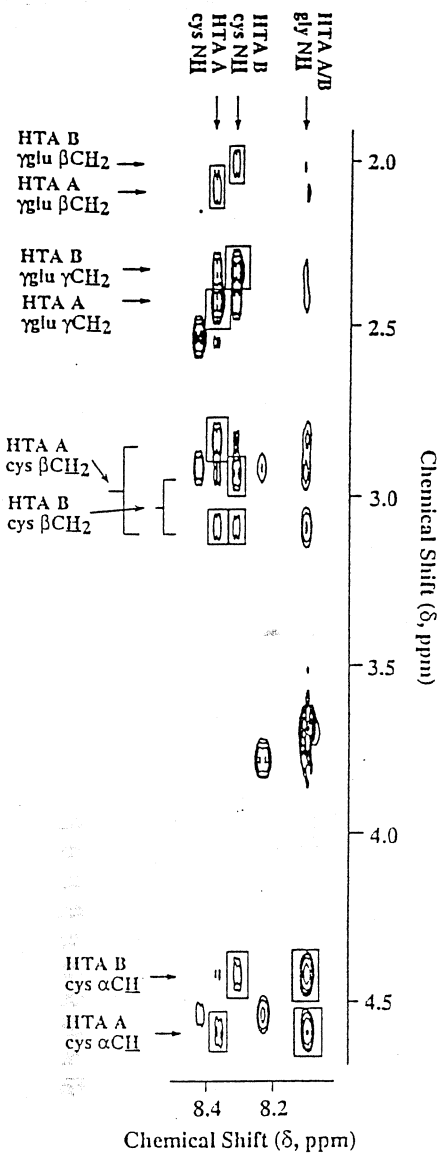

FIGURE 4: Part of the 600.14-MHz NOESY spectrum of phenylglyoxal and GSH acquired at pH* 4.4 and 303 K. The sample contained ~200 mM GSH and phenylglyoxal constituted in H_2O (10% ^2H_2O v/v) and the pH* was adjusted with 10 M NaOH. The spectrum was derived from 400 spectra of 64 transients each, collected over 2K data points and transformed with one degree of zero filling using a shifted sine bell ($\theta = \pi/2$) in both the $F1$ and $F2$ dimensions. The intense water signal was suppressed by presaturation. Notes on assignments: The assignments are as shown. The unassigned columns of peaks arise from (in order of increasing frequency in the $F2$ domain) GSH gly-NH and GSH cys-NH. The intense peak at δ 8.1, 3.7 arises from both hemithioacetals and is a NOE cross-peak between gly NH and gly αCH. There are also "exchange" NOE cross peaks which arise because the diastereomers are in rapid chemical exchange during the long mixing time, 0.95 s.

cross-peak volumes were measured for each form. When the volumes were converted into approximate upper limits of internuclear distance it became apparent that there was no significant difference between the diastereomers at this level of resolution. Therefore, using this single list of 33 "consensus" distances together with 45 lower limit non-NOE constraints (see Materials and Methods), 1000 structures were computer-generated using the DSA protocol. Two hundred and forty-five of these structures converged to an "acceptable" total potential energy of 125–170 kJ mol^{-1}, the rest had a much higher energy (250–670 kJ mol^{-1}; this can be largely accounted for by an increase in angle energy indicating that the high-energy structures had nonideal geometry. Note that these energies must be positive since the nonbonded (repel) term

Table 1: Agreement between Predicted and Observed Chemical Shift Values[a]

	R			S	
χ_{min} (%)	A or B	E_{total}	χ_{min} (%)	A or B	E_{total}
27	B	32.5	33	A	32.8
33	B	31.0	37	A	33.1
34	B	30.8	38	A	32.2
39	B	31.7	38	A	33.7
42	B	31.5	38	A	33.8
43	B	30.8	42	A	32.1
44	B	30.9	43	A	32.2
46	B	30.7	45	B	39.1
49	B	32.7	48	A	33.2

[a] The table lists all HTA structures with χ_{min} values of 50% or less for both the R and S diastereomers. The "A or B" column indicates with which spectral form the predicted chemical shifts agreed more closely. The E_{total} column indicates the final total potential energy of each structure at the end of the DSA procedure. (Clearly, the R diastereomer gives much better agreement to the B form, whereas the S diastereomer fits better to the A form, suggesting very strongly that the B form can be assigned to the R diastereomer and vice versa; see Discussion.)

used does not have any attractive (–ve energy) component and replaces the normal van der Waals and electrostatic terms). Of the 245 low energy structures, 178 were R diastereomers, and 67 were S. For each of these structures the ring current chemical shifts were then calculated and a goodness of fit to the observed values for the A (χ_A) and B (χ_B) forms was assessed (using an expression akin to eq 4). The calculated structures were then ranked in order of $\chi_{min} = \min(\chi_A,\chi_B)$ (Table 1); Table 1 shows all structures which had χ_{min} values of greater than 50% (nine structures each for the R and S diastereomers). Thus, Table 1 shows that the R diastereomer gave much better agreement with the B form of the HTA, whereas the S diastereomer fitted better to the A form of the HTA. This correlation strongly suggests that the B form is the R diastereomer and the A form is the S diastereomer.

In the 600.14-MHz NOESY spectrum of methylglyoxal and GSH (not shown), NOE cross peaks were detected for 35 out of a total of 55 possible interactions between the 11 resolved diagonal peaks. In the few cases where NOE peaks from the two diastereomers were resolved, the integrals of these peaks were combined to give peak volumes equivalent to those where the peaks were not resolved. Using 35 upper limit NOE constraints and 20 lower limit non-NOE constraints, the DSA procedure generated 1000 structures for methylglyoxal-HTA; 266 of these structures converged to a total energy of 56–147 kJ mol^{-1}; the rest of the structures were trapped in local minima of higher energy (250–690 kJ mol^{-1}).

Figure 5 shows, overlaid, the seven best R and S phenylglyoxal-HTA structures selected on the basis of the lowest χ_{min}, and the seven best methylglyoxal-HTA structures, selected on the basis of lowest overall potential energy. In each case, the structures have been superimposed onto the "best" (least energy) structure. Note that the structures have the same Y-shape with respect to the orientation of the γ-glutamyl and the glycyl. However, the R and S forms differ with respect to the orientation of the cysteinyl side chain in relation to the backbone Y-shape. The orientation of this side chain in methylglyoxal-HTA appears to be closer to that of the S form of phenylglyoxal-HTA than the R form.

The concentration ratios of the diastereomers were derived from the integrals of the HTA methine protons in "fully-relaxed" ^{1}H NMR spectra. For phenylglyoxal-HTA the equilibrium ratio was 1:1.016 (A/B) at pH* 4.4 (49.6% minor isomer). The forward rate of interconversion was measured

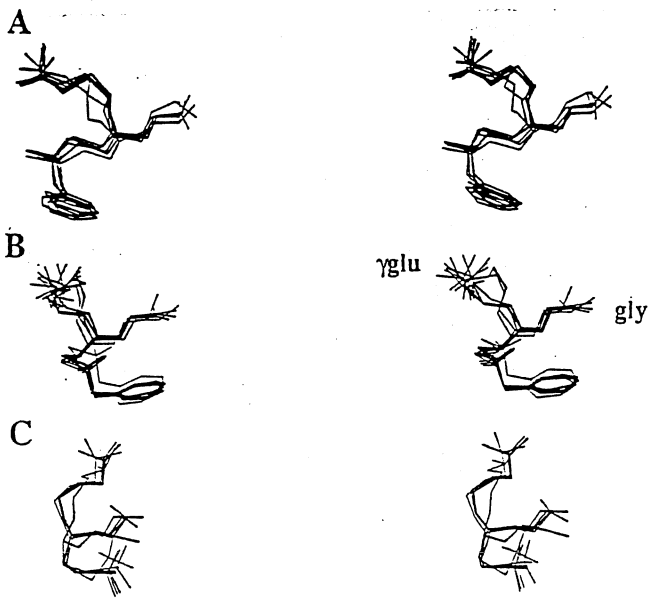

FIGURE 5: Structures of phenylglyoxal-HTA and methylglyoxal-HTA diastereomers generated by using dynamical simulated annealing. Stereoviews of the seven best HTA(*R*) and -(*S*) structures (A and B, respectively), selected on the basis of the best fit to the observed chemical shifts (see Table 1), and the seven best methylglyoxal-HTA structures (C), selected on the basis of overall potential energy. In each case, the structures were superimposed onto the "best" (minimum energy) structure.

using magnetization transfer (see Materials and Methods) to be 0.30 ± 0.04 s^{-1} (±sd). In the case of methylglyoxal, the equilibrium concentration ratio was 1:0.927 (A/B; 48.1%minor isomer) and the forward rate constant was measured to be 0.15 ± 0.02 s^{-1}.

The effect of adding large amounts (~200 units) of glyoxalase 1 to a ~200 mM solution of phenylglyoxal and GSH is shown in Figure 6A. One of the acetal methine proton resonances of phenylglyoxal-HTA declined at a faster rate than the other. The difference in the intensities of the methine protons with time can be seen more clearly in the inset graph in Figure 6A. In the case of methylglyoxal-HTA, however, the stereoselectivity in rate of decline was not seen (Figure 6B); the two methine singlets disappeared at apparently identical rates (inset to Figure 6B). Note that the methine singlets in the methylglyoxal-HTA were not of equal initial intensity as opposed to the case with the phenylglyoxal-HTA (see above).

The results of computer modeling the reaction schemes in eq 1–3 are shown in Figure 7. Figure 7A shows the results of simulating the scheme shown in eq 1, where glyoxalase 1 acts on the hemithioacetal diastereomers formed from *phenyl*glyoxal and GSH, and the same situation with methylglyoxal and GSH is shown in Figure 7B. The rate constants characterizing the chemical interconversion of the two diastereomers, measured in magnetization transfer experiments (see above), were used together with V_{max} calculated from the known amount of glyoxalase 1 used in the experiment (Figure 6A) and the published K_M value (Vander Jagt *et al.*, 1972). The slower rate of interconversion of the methylglyoxal-HTA resulted in an even greater predicted differential metabolism of the diastereomers than that seen for phenylglyoxal-HTA (Figure 7A).

A similar series of time courses was obtained for the simulation of the metabolism of phenylglyoxal-HTA using the scheme shown in eq 2 (Figure 7C) for which the relative V_{max} values of the enzyme acting on each diastereomer were

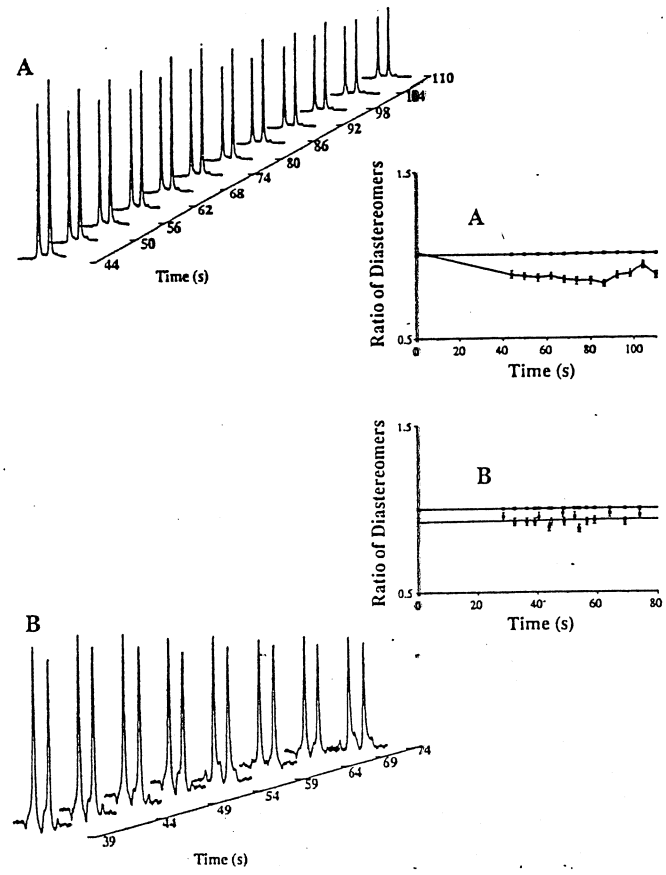

FIGURE 6: Time courses showing isomerization of hemithioacetals by glyoxalase 1. Part A shows the effect of adding excess glyoxalase 1 to a mixture of phenylglyoxal and GSH at pH* 4.4. The sample contained ~200 mM phenylglyoxal and 200 mM GSH in ^2H_2O adjusted to pH* 4.4 using NaO^2H (0.65 mL total volume). One hundred and fifty microliters of enzyme solution was added at zero time (500 units of glyoxalase 1 in 400 μL ^2H_2O). Each spectrum was derived from the sum of two transients and was acquired at 400.13 MHz. The resonances shown are from the methine protons of both hemithioacetals which are separated by 20.9 Hz. The inset graph shows the intensity of resonance A (Figure 2) (□) compared with that of B (■) set to 1 at each point in the time course. The zero time point was taken from an initial spectrum of the same solution. Error bars denote the standard error obtained when estimating the intensity of the resonances with respect to the noise. Part B shows the effect of adding excess glyoxalase 1 to a mixture of methylglyoxal and GSH at pH* 4.4. The sample contained ~200 mM GSH and ~200 mM methylglyoxal. Thirty-four microliters of glyoxalase 1 solution (500 units in 400 μL of ^2H_2O) was added to the tube at zero time and spectra of one transient each were recorded, beginning as soon as possible after starting the reaction. The peaks shown are the methine resonances (separation 14.2 Hz) from both hemithioacetals. The inset graph shows the intensity of resonance B (Figure 3) (□) compared with that of A (■) set to 1 at each point in the time course. The data points were obtained from two separate experiments. Error bars denote the standard error obtained when estimating the intensity of the resonances with respect to the noise.

varied to yield a visual fit to the experimentally measured disappearance of the diastereomeric substrate. Repeated-simulations of the reaction using the enzyme and substrate concentrations employed in the NMR experiments, revealed that the simulated rate was relatively insensitive to alterations in the value of K_M; altering K_M by a factor of 1000 had only a very slight effect on the simulated timecourse (see Figure 7D).

The results of simulating the reaction scheme shown in eq 3 are shown in Figure 7, parts E and F. The simulated time course in Figure 7E mimics that in the real experiment (Figure 6A). The experimentally measured rate of interconversion of the two diastereomers of phenylglyoxal-HTA was used in the

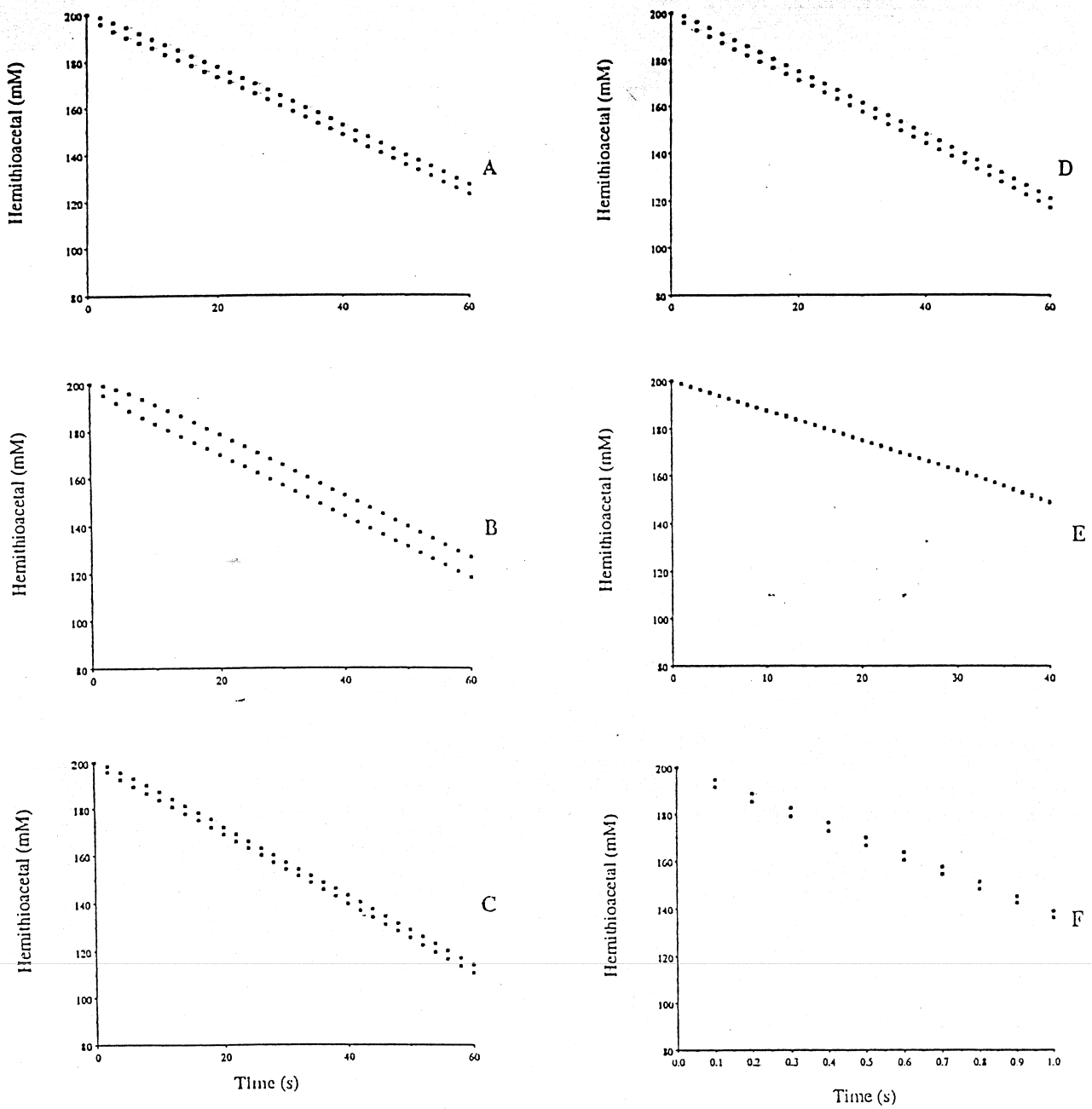

FIGURE 7: Computer-based simulations of HTA consumption by glyoxalase 1 under various conditions based on the reaction schemes depicted in eqs 1–3. (A) the scheme used was that shown in eq 1. Parameter values: $k_1 = k_{-1} = 0.3\ s^{-1}$ (this was the measured interconversion rate of phenylglyoxal diastereomers), $V_{max} = 2.5$ mmol $L^{-1}\ s^{-1}$, $K_M = 0.2$ mM (standard parameters for the amount of yeast enzyme added). (B) The scheme used was that shown in eq 1. Values: $k_1 = k_{-1} = 0.15\ s^{-1}$ (measured interconversion rate of methylglyoxal diastereomers), $V_{max} = 2.577$ mmol $L^{-1}\ s^{-1}$, $K_M = 0.2$ mM (standard parameters for the amount of yeast enzyme added). (C) The scheme used was that shown in eq 2. Values: $k_1 = k_{-1} = 0.3\ s^{-1}$ (measured interconversion rate of phenylglyoxal diastereomers), $V_{max1} = 2.5$ mmol $L^{-1}\ s^{-1}$, $K_{M1} = 0.2$ mM (standard parameters for the amount of yeast enzyme added), $V_{max2} = 0.3$ mmol $L^{-1}\ s^{-1}$, $K_{M2} = 0.2$ mM. (D) Scheme used is that shown in eq 2. Values used are as in C (above) except for $K_{M2} = 200$ mM. (E) Scheme used is that shown in eq 3. Values: $k_1 = k_{-1} = 0.3\ s^{-1}$ (measured interconversion rate of phenylglyoxal diastereomers), $k_2 = k_{-2} = 4.83 \times 10^5\ s^{-1}$ (100 times the measured chemical interconversion rate), $k_3 = k_4 = 2.4976 \times 10^5$ L $mol^{-1}\ s^{-1}$, $k_{-3} = k_{-4} = 1.00 \times 10^5\ s^{-1}$ (assuming all but $\sim 1/1000$ of the enzyme is in the bound form and that the rate constant characterizing the binding is $\sim 10^5$ L $mol^{-1}\ s^{-1}$, a conservative estimate), $k_5 = 200\ s^{-1}$ (calculated on the basis of k_{cat} *i.e.*, to convert substrate to product at the rate observed experimentally), initial enzyme concentration, $E_0 = 25\ \mu M$ (the amount of enzyme used in the experiment shown in Figure 4A); k_3, k_4 and k_{-3}, k_{-4}, were made equal, as small variations were unlikely to manifest themselves significantly in the time course because k_3, $k_4 \gg k_{cat}$. (F) The scheme used was that shown in eq 3. Values (second-order rate constants have units of L $mol^{-1}\ s^{-1}$, while first-order constants have the units s^{-1}): k_1, k_{-1}, k_3, k_4, k_{-3}, k_{-4}, and k_5 unchanged from E (above); $k_2 = 4.805 \times 10^3$ (100 times the measured chemical interconversion rate); $E_0 = 1.25$ mM, *i.e.*, 50 times that used in graph E above.

model, the k_{cat} was set so as not to exceed that which was experimentally attained; the latter value was related to the amount of enzyme used. The rate of the putative enzyme-catalyzed interconversion of the hemithioacetals was set conservatively to be only 100 times faster than the nonenzymic rate, although many enzyme-catalyzed reactions have rate-enhancement factors much greater than this (*e.g.*, Price & Stevens, 1989). Thus, the rate-limiting step of the overall reaction would no longer be the rate of nonenzymic interconversion of the hemithioacetals. Consequently, no stereospecific preference was seen in the simulated time course (Figure 7E). When the simulated reaction was made to proceed faster by increasing the concentration of the enzyme, the stereospecific preference seen experimentally was observed. However, the overall rate of product formation was greater, with the increase being proportional to the amount of additional

enzyme; in this situation the simulation predicted that the reaction would be complete in only a few seconds (Figure 7F).

DISCUSSION

Discriminating between Kinetic Schemes: Equations 1 and 2. Deciding if the reaction schemes, eqs 1 or 2, apply to experimental reality was achieved by comparing simulated time courses with the corresponding experimental data. When the overall glyoxalase 1 reaction was simulated using the scheme in eq 1, with phenylglyoxal-HTA as substrate, the time course of reactant concentrations was as shown in Figure 7A. However, there was an even greater differential usage of diastereomers seen with methylglyoxal-HTA (Figure 7B). This outcome was deemed to be a consequence of the facts that (1) the experimentally measured rate of nonenzymic interconversion of the methylglyoxal HTA diastereomers is slower than that of the phenylglyoxal-HTA diastereomers and; (2) glyoxalase 1 displays a greater V_{max} (turnover number) for methylglyoxal-HTA than for phenylglyoxal-HTA; the relative maximal rates are 1.0:0.93 in the case of the yeast enzyme (Vander Jagt *et al.*, 1972).

Experimentally, the diastereomers of methylglyoxal-HTA were consumed at rates which were not detectably different (Figure 6B). Therefore eq 1 can be rejected as the overall mechanism of the reaction. In other words, glyoxalase 1 appears to operate with equal reaction rate on *both* methylglyoxal-HTA diastereomers and this is explicitly not included in the scheme of eq 1. The report of Griffis *et al.* (1983), on the conversion of both diastereomers of phenylglyoxal by glyoxalase 1, and also the work of Landro *et al.* (1992), who used NMR to monitor the direct conversion of stereochemically "locked" substrate analogues, support this argument.

Discriminating between Kinetic Schemes: Equations 2 and 3. Discriminating between the kinetic characteristics of the schemes outlined in eqs 2 and 3 is more complex than for the case above. In order to experimentally demonstrate stereopreference in the reaction scheme outlined in eq 2, the reaction must proceed sufficiently rapidly that the rate of nonenzymic interconversion of the stereoisomers is slower than that of the enzyme-catalyzed reaction; this will allow any preferential usage to be manifest. In fact, this was achieved experimentally as shown in Figure 6A. Simulation of the scheme using known parameters (k_1 and k_{-1}, determined in this work) and reasonable estimates of parameters (V_{max} and K_M), is shown in Figure 7C.

In the case of eq 3, differential consumption of diastereomers can be achieved in one of two ways. The first possibility is if the rate of the enzyme-catalyzed interconversion of substrates (k_2) approximates that of the nonenzymic interconversion (k_1); when this situation was simulated, differential metabolism of the stereoisomers was observed. However, the progress curve (not shown) of substrate consumption followed a sigmoidal form rather than the experimentally observed linear one (Figure 6A); the former is a typical outcome for a two-or-more step reaction [*e.g.*, Kuchel (1985)]. Additionally, enzyme-catalyzed reactions are usually several orders of magnitude faster than the corresponding nonenzymic reaction, and indeed, may increase the rate of a reaction by as much as 10^{14}-fold [*e.g.*, Price and Stevens (1989)].

The second, more likely, way an observed stereopreference may be rationalized by eq 3 is if the rate of enzyme-catalyzed product formation (k_5) proceeds faster than the rate of enzyme-catalyzed isomerization of substrate (k_2). Accordingly, in order to show stereopreferential disappearance of substrate to the extent seen experimentally with phenylglyoxal-HTA, the enzymic reaction must be made to proceed ~50 times faster (or the enzyme concentration must be 50 times larger) than in the experiment (Figure 6A). The simulations in Figure 7, parts E and F, demonstrated that the scheme shown in eq 3 is also not an adequate description of the experimental data.

Implicit in the hypothesis that the enzyme catalyzes the interconversion of the hemithioacetal diastereomers is the assumption that the enzyme can also bind GSH separately to the α-keto aldehyde, as has been suggested (Mannervik *et al.*, 1974; Marmstal & Mannervik, 1981). Other kinetic studies, however, do not support this proposal (Vander Jagt *et al.*, 1975; Rae *et al.*, 1990).

Simulation of the reaction scheme of eq 3 required estimation of values for the many parameters, and these were chosen to be "consistent" with the fact that enzyme-catalyzed diastereomeric interconversion ought to be at least 2 orders of magnitude faster than nonenzymic interconversion. Additionally, those parameters describing binding of substrate to enzyme (k_3,k_4) were given conservatively low [*e.g.*, Price and Stevens (1989)] values (~10^5 s^{-1}) and in the interests of simplicity they were made equal (Figure 7E). Even if the enzyme binds one of the diastereomers preferentially (*viz.* $k_3 > k_4$), both of these rate constants would still be several orders of magnitude greater than the rate constant characterizing product formation (k_5) which approximates to V_{max}/(total enzyme concentration) = k_{cat}. Thus the present argument suggests that the enzyme does not catalyze the interconversion of the diastereomers; it must be operating on each diastereomer separately.

A Model for the Glyoxalase 1 Reaction. On the basis of the above arguments, relating to the comparison between experimental results and computer simulations and considering the mechanisms proposed previously (Kozarich & Chari, 1982; Chari & Kozarich, 1983; Landro *et al.*, 1992), a possible scheme for the glyoxalase reaction which considers the information available to date is as follows:

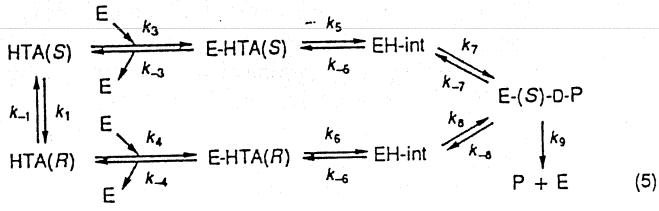

(5)

where k_5 and k_6 characterize the rate of abstraction of the methine proton from each enzyme-bound diastereomer, and k_7 and k_8 characterize the rate of stereospecific reprotonation at the carbon adjacent to that from which the previous abstraction took place. EH-int represents the enzyme bound intermediate with an abstracted proton and E-(*S*)-D-P the enzyme-bound product. The rate constant that characterizes the release of product by the enzyme is denoted by k_9. The steps of the entire reaction which are primarily "rate limiting" are those characterized by k_5 and k_6, or k_7 and k_8, rather than k_9; this is a requirement for the manifestation of stereopreference. The values of k_5, k_6, k_7, and k_8 were first made to approximate k_{cat}, and then, by adjusting these values, it was possible to obtain a graph of stereoisomer metabolism similar to that seen in Figure 7C, which is very similar to that observed experimentally (Figure 6A).

Computer simulation of the scheme shown in eq 2 illustrates that, at the high substrate concentrations used experimentally, the reaction rate is insensitive to the K_M (Figure 7, parts C and D). This can be readily explained: since the initial substrate concentration is ~3 orders of magnitude greater

than K_M, then for a large extent of the reaction the rate will be very close to the maximal velocity of the enzyme. In this situation, changes in the rate of product formation will occur only as a result of changes in V_{max}, rather than K_M; this can be rationalized as follows.

The simplest of all enzyme-catalyzed reactions can be represented by

$$E + S \underset{k_{-1}}{\overset{k_1}{\rightleftharpoons}} ES \xrightarrow{k_2} E + P \quad (6)$$

where E corresponds to enzyme, S substrate, and P product. In steady-state analysis of the kinetics, the initial substrate concentration is taken to be much greater than the enzyme concentration; K_M is identified with $(k_{-1} + k_2)/k_1$, and V_{max} with k_2E (Price & Stevens, 1989). Since k_1 and k_{-1} are considered to be large relative to k_2, a change in k_2 does not result in appreciable changes in K_M, although it obviously directly affects V_{max}.

With these concepts in mind it can be concluded that the different rates of conversion seen for the phenylglyoxal-HTA diastereomers are due to different values of k_{cat}, which characterize different rates of formation and breakdown of the transition-state complexes, rather than the binding process (characterized by k_1) *per se*. Previously obtained results (Vander Jagt *et al.*, 1972) also support this conclusion: for a given glyoxalase 1 concentration, methylglyoxal has a greater V_{max} than phenylglyoxal (1.0 vs 0.93 for the yeast enzyme), but the reported K_M values for some substituted phenylglyoxal hemithioacetals are *lower* than that for methylglyoxal (3×10^{-4} M for methylglyoxal *cf.* 2×10^{-5} M for chloro- and phenyl-*para*-substituted phenylglyoxal). Thus the apparent binding affinity between the enzyme and the substrate increases with the size and hydrophobic nature of the substituents (Vince & Wadd, 1969; Vince *et al.*, 1971; Vander Jagt *et al.*, 1972). This has led to the suggestion of the existence of a hydrophobic pocket at or near the binding site of glyoxalase 1. More recently, Landro *et al.* (1992) concluded that the slow processing of glutathiohydroxyacetone by glyoxalase 1 is *not* due to weak binding, as this molecule proved to be a good competitive inhibitor of glyoxalase 1, and therefore, the chemical transformation steps are what differ in rate between the stereospecific substrates.

The broad range of α-keto aldehydes susceptible to glyoxalase 1 is in keeping with its suggested role as a broad-spectrum detoxifier of these compounds: the enzyme accepts methylglyoxal, phenylglyoxal (Dakin & Dudley, 1913), hydroxymethylglyoxal (Reeves & Ajl, 1965), and hydroxymethylglyoxal phosphate (Weaver & Lardy, 1961) as well as glyoxal and many other alkyl- and arylglyoxals (Vander Jagt *et al.*, 1975). The specificity of glyoxalase 1 for GSH, on the other hand, is high; apart from *N*-acyl derivatives of GSH, and several related tripeptides, other molecules containing sulfydryl groups are inactive, primarily due to poor enzyme-binding affinity (Kozarich & Chari, 1982). The importance of the γ-glutamyl moiety in the binding process has been shown in studies on the effect of GSH substitution: GSH may be replaced by α-L-glu-L-cys-gly, β-L-asp-L-cys-gly and γ-D-glu-L-cys-gly; but, all these compounds are less effective than GSH as a substrate (Kermack & Matheson, 1957). While γ-L-glu-L-cys and L-cys-gly are not effective, γ-L-glu-L-cys-β-ala reacts at a rate that is 55% that of GSH, under optimal conditions for each substrate (Carnegie, 1963). It was suggested (Schasteen & Reed, 1983) that the glycyl carboxylate is essential in the binding process, but this has since been disputed by Hamilton and Creighton (1992) who observed that glycylmethyl and glycylethyl esters of methylglyoxal-HTA will serve as moderately efficient substrates for glyoxalase 1.

The preference of the enzyme for GSH may be related to its essential "shape", an extended Y structure (Laurence & Thomson, 1980; Podányi & Reid, 1988), a conformation which appears to be maintained when bound to glyoxalase 1 (Rosevear *et al.*, 1984).

Xie and Creighton (1991) synthesized glutathione with a methyl group substituted for either H_R or H_S of cys βCH_2 and concluded that the spatial requirement of the cys Cβ-H_S proton is a strict requirement for productive substrate binding. Interestingly, the cys βCH_2 and acetal CHOH of both the phenylglyoxal-HTA(*S*) and the methylglyoxal-HTA structures generated in this work have similar orientation, being "cis" to one another, while these groups in the phenylglyoxal-HTA(*R*) are "trans".

The Conformation of the Hemithioacetal Substrate. This work has revealed a distinctly different conformation for each of the hemithioacetal diastereomers formed between phenylglyoxal and GSH. The one-dimensional 600.14-MHz ^1H NMR spectrum of the diastereomers formed between phenylglyoxal and GSH has distinct resonances for all of the protons in each diastereomer (Figure 2). The differences in chemical shifts are attributable to shielding caused by local magnetic fields induced by the delocalized π-electrons of the phenyl ring (Pauling, 1936). The resultant chemical shift is thus related to the spatial position of the nucleus with respect to the plane of the ring (Johnson & Bovey, 1958); the ring having a different average orientation in each diastereomer.

Ideally, the chemical-shift-energy (Zeeman energy) term should be included in the force field used in the DSA analysis. In the absence of the ability of the present program (X-PLOR 3.0) to include this term, a large set of structures were generated, and those which agreed best with the observed chemical shifts were selected. Thus it was possible to assign the A and B forms, as named in the spectra, to the *S* and *R* diastereomers, respectively. Glyoxalase 1 thus appears to display no distinguishable stereopreference; preferring the *S* diastereomer of phenylglyoxal HTA, neither diastereomer of methylglyoxal-HTA and the *R* diastereomer of glutathiolactaldehyde. This also suggests that the overall orientation of the diastereomer is more important than the actual stereochemistry.

A deviation from precise stereospecific product formation by glyoxalase 1 was demonstrated by Kozarich and Chari (1982) using an "inverted" substrate, glutathiomethylglyoxal, a molecule which possesses a free aldehyde group. Attaching thiols other than GSH, such as ethanethiol and β-mercaptoethanol, to this aldehyde resulted in inverted processing of the substrate, thus yielding the L-isomer of lactate. Glutathiomethylglyoxal conjugated with GSH, however, produced the normal D-lactate. In addition, another recent report (McClellan & Thornalley, 1991) indicates that glyoxalase 1 produces the (*S*)-L-isomer of glyceroylglutathione when metabolizing hydroxymethylglyoxal; this conclusion was based on the detection of L-glycerate after hydrolysis of the product by glyoxalase 2. This was the first report of the measurement of the angle of optical rotation of the product of glyoxalase metabolism with hydroxymethylglyoxal as substrate, and the only report of the production of an L-isomer from the metabolism by the glyoxalases of α-keto aldehydes. The optical purity of recovered glycerate was only 72 ± 10% compared with 97 ± 7 and 99 ± 3% for D-mandelate and

D-lactate, the products of metabolism of phenylglyoxal and methylglyoxal by the glyoxalase enzymes, respectively. Possible racemization of glyceroylglutathione and glycerate was minimized by judicious choice of experimental conditions. However, in an earlier paper (Patterson *et al.*, 1981) where it is suggested the conditions used could have favored racemization, the yields of optical isomers for lactate and mandelate were similar.

Production by glyoxalase 1 of the L-optical isomer from hydroxypyruvaldehyde was rationalized by McClellan and Thornalley (1991) on the basis that a hydroxymethyl group is hydrophilic compared with a methyl or phenyl group; this causes a change in the alignment of the molecule in the active site. However, hydroxymethylglyoxal phosphate, which is very hydrophilic, is metabolized by the glyoxalase enzymes to D-phosphoglycerate (Weaver & Lardy, 1961) with a measured isomeric optical purity of 98%. Hydroxymethylglyoxal is among the most chemically unstable of the α-keto aldehydes (Wolff *et al.*, 1984) readily breaking down, via enediol intermediates, in a series of oxidation–decarboxylation reactions to yield formate. The acid intermediates in the reaction constitute a racemic mixture in the breakdown process. Also, α-keto aldehydes are known to form the corresponding hydroxy acid spontaneously in a reaction which is accelerated at alkaline pH and which results in a racemic mixture (Weaver & Lardy, 1961). Further investigation of hydroxymethylglyoxal, a comparatively poor substrate for glyoxalase 1, is warranted.

In conclusion, glyoxalase 1 appears to metabolize, with equal avidity, the *R* and *S* forms of methylglyoxal-HTA while it favors one form of the phenylglyoxal-HTA. The methods used here have overcome the technical difficulties associated with experiments on a mixture of interconverting diastereomers. Identification of the preferred diastereomer required the assignment of the ^{1}H NMR spectra of the diastereomers of the hemithioacetals using contemporary 2D NMR and computer modeling techniques; these assignments depended in an important way on the quantitative analysis of ring-current shifts. Thus, it was deduced that it is the *S* form of phenylglyoxal-HTA which is used preferentially by the enzyme. Further studies of the mechanism of, and the diversity of substrates metabolized by, the two glyoxalases will contribute to the determination of the roles of this ubiquitous enzyme system.

ACKNOWLEDGMENT

Drs. Sue Berners-Price and Glenn King are thanked for valuable discussions. Messrs. Bill Lowe and Brian Bulliman are thanked for expert technical and computing assistance, respectively. Drs. Kirk Marat and Rudy Sebastian, Department of Chemistry, University of Manitoba, Winnipeg, Canada, are thanked for providing NUMARIT.

REFERENCES

Bax, A., Griffey, R. H., & Hawkins, B. L. (1983) *J. Magn. Reson. 55*, 301–315.

Braun, W., Bösch, C., Brown, L. R., Gō, N., & Wüthrich, K. (1981) *Biochim. Biophys. Acta 667*, 377–396.

Brown, C., Douglas, K. T., & Ghobt-Sharif, J. (1981) *J. Chem. Soc., Chem. Commun.* 944–946.

Brunger, A. T. (1992) *X-PLOR Version 3.0, User manual*, Yale University, New Haven, CT.

Carnegie, P. R. (1963) *Biochem. J. 89*, 471–478.

Chari, R. V. J., & Kozarich, J. W. (1982) *J. Biol. Chem. 256*, 9785–9788.

Chari, R. V. J., & Kozarich, J. W. (1983) *J. Am. Chem. Soc. 105*, 7169–7171.

Dakin, H. D., & Dudley, H. W. (1913) *J. Biol. Chem. 14*, 423–431.

Douglas, K. T., Quilter, J. A., Shinkai, S., & Ueda, K. (1985) *Biochim. Biophys. Acta 829*, 119–126.

Ekwall, K., & Mannervik, B. (1973) *Biochim. Biophys. Acta 297*, 297–299.

Ferrin, T., Huang, C. C., Jarvis, L. E., & Langridge, R. (1988) *J. Mol. Graphics 6*, 13–27.

Frazen, V. (1956) *Chem. Ber. 89*, 1020.

Gear, C. W. (1969) in *Information Processing 68* (Morrell, A. J. H., Ed.) pp 187–193, North Holland, Amsterdam.

Griffis, C. E. F., Ong, L. H., Beuttner, L., & Creighton, D. J. (1983) *Biochemistry 22*, 2945–2951.

Hall, S. S., Doweyko, A. M., & Jordan, F. (1976) *J. Am. Chem. Soc. 98*, 7460–7461.

Hall, S. S., Doweyko, A. M., & Jordan, F. (1978) *J. Am. Chem. Soc. 100*, 5934–5939.

Hamilton, D. S., & Creighton, D. J. (1992) *Biochim. Biophys. Acta 1159*, 203–208.

Johnson, C. E., & Bovey, F. A. (1958) *J. Chem. Phys. 29*, 1012–1014.

Kellum, M. W., Oray, B., & Norton, S. J. (1978) *Anal. Biochem. 85*, 586–590.

Kermack, W. O., & Matheson, N. A. (1957) *Biochemistry 65*, 48–58.

Kozarich, J. W., & Chari, R. V. J. (1982) *J. Am. Chem. Soc. 104*, 2655–2657.

Kozarich, J. W., Chari, R. V. J., Wu, J. C., & Lawrence, T. L. (1981) *J. Am. Chem. Soc. 103*, 4593–4595.

Kuchel, P. W. (1985) in *Kinetic Analysis of Organized Multienzyme Systems* (Welch, G. R., Ed.) pp 303–380, Academic Press, Orlando.

Kumar, A., Ernst, R. R., & Wüthrich, K. (1980) *Biochem. Biophys. Res. Commun. 95*, 1–6.

Landro, J. A., Brush, E. J., & Kozarich, J. A. (1992) *Biochemistry 31*, 6069–6077.

Laurence, P. R., & Thomson, C. (1980) *Theor. Chim. Acta 57*, 25–41.

Mannervik, B., Bartfai, I., & Gorna Hall, B. (1974) *J. Biol. Chem. 249*, 901–903.

Marmstal, E., & Mannervik, B. (1981) *FEBS Lett. 131*, 301–304.

McClellan, J. D., & Thornalley, P. J. (1991) *J. Chem. Soc., Perkin Trans. 1* 3009–3015.

Nilges, M., Clore, G. M., & Gronenborn, A. M. (1988) *FEBS Lett. 239*, 129–136.

Patterson, A. K., Szajewski, R. P., & Whitesides, G. M. (1981) *J. Org. Chem. 46*, 4682–4685.

Pauling, L. (1936) *J. Chem. Phys. 4*, 673–677.

Perrin, C. L., & Engler, R. E. (1990) *J. Magn. Reson. 90*, 363–369.

Piantini, U., Sorensen, O. W., & Ernst, R. R. (1982) *J. Am. Chem. Soc. 104*, 6800–6801.

Podányi, B., & Reid, R. S. (1988) *J. Am. Chem. Soc. 110*, 3805–3810.

Price, N. C., & Stevens, L. (1989) in *Fundamentals of Enzymology*, Chapter 4, p 4, Oxford Science Publications, Oxford, UK.

Quirt, A. R., & Martin, J. S. (1971) *J. Magn. Reson. 5*, 318–327.

Racker, E. (1951) *J. Biol. Chem. 190*, 685–696.

Rae, C., Berners-Price, S. J., Bulliman, B. T., & Kuchel, P. W. (1990) *Eur. J. Biochem. 193*, 83–90.

Reeves, H. C., & Ajl, S. J. (1965) *J. Biol. Chem. 240*, 569–573.

Robinson, G., Kuchel, P. W., Chapman, B. E., Doddrell, D. M., & Irving, M. G. (1985) *J. Magn. Reson. 63*, 314–319.

Rose, I. (1957) *Biochim. Biophys. Acta 25*, 214–215.

Rosevear, P. R., Sellin, S., Mannervik, B., Kuntz, I. D., & Mildvan, A. S. (1984) *J. Biol. Chem. 259*, 11436–11447.
Schasteen, C. S., & Reed, D. J. (1983) *Biochim. Biophys. Acta 742*, 419–425.
Sellin, S., & Mannervik, B. (1983) *J. Biol. Chem. 258*, 8872–8875.
Shaka, A. J., Keeler, J., & Freeman, R. (1983) *J. Magn. Reson. 53*, 313–340.
Shinkai, S., Yamashita, T., Kusano, Y., & Manabe, O. (1981) *J. Am. Chem. Soc. 103*, 2070–2074.
Vander Jagt, D. L., Han, L.-P. B., and Lehmann, C. H. (1972) *Biochemistry 11*, 3735–3740.
Vander Jagt, D. L., Daub, E., Krohn, J. A., & Han, L. B. (1975) *Biochemistry 14*, 3669–3675.
Vince, R., & Wadd, W. B. (1969) *Biochem. Biophys. Res. Commun. 35*, 593–598.
Vince, R., Daluge, S., & Wadd, W. B. (1971) *J. Med. Chem. 14*, 402–404.
Weaver, R. H., & Lardy, H. A. (1961) *J. Biol. Chem. 236*, 313–317.
Wolff, S. P., Crabbe, M. J. C., & Thornalley, P. J. (1984) *Experientia 40*, 244–246.
Xie, X., & Creighton, D. J. (1991) *Biochem. Biophys. Res. Commun. 177*, 252–258.